Interaction of Group IA Phospholipase A_2 with Metal Ions and Phospholipid Vesicles Probed with Deuterium Exchange Mass Spectrometry†

John E. Burke,‡ Mark J. Karbarz,‡ Raymond A. Deems,‡ Sheng Li,§ Virgil L. Woods, Jr.,*,§ and Edward A. Dennis*,‡

Department of Chemistry and Biochemistry and Department of Pharmacology, School of Medicine, and Department of Medicine and Biomedical Science Graduate Program, School of Medicine, University of California at San Diego, La Jolla, California 92093-0601

Received January 17, 2008; Revised Manuscript Received April 25, 2008

ABSTRACT: Deuterium exchange mass spectrometric evaluation of the cobra venom (*Naja naja naja*) group IA phospholipase A_2 (GIA PLA_2) was carried out in the presence of metal ions Ca^{2+} and Ba^{2+} and phospholipid vesicles. Novel conditions for digesting highly disulfide bonded proteins and a methodology for studying protein−lipid interactions using deuterium exchange have been developed. The enzyme exhibits unexpectedly slow rates of exchange in the two large α-helices of residues 43−53 and 89−101, which suggests that these α-helices are highly rigidified by the four disulfide bonds in this region. The binding of Ca^{2+} or Ba^{2+} ions decreased the deuterium exchange rates for five regions of the protein (residues 24−27, 29−40, 43−53, 103−110, and 111−114). The magnitude of the changes was the same for both ions with the exception of regions of residues 24−27 and 103−110 which showed greater changes for Ca^{2+}. The crystal structure of the *N. naja naja* GIA PLA_2 contains a single Ca^{2+} bound in the catalytic site, but the crystal structures of related PLA_2s contain a second Ca^{2+} binding site. The deuterium exchange studies reported here clearly show that in solution the GIA PLA_2 does in fact bind two Ca^{2+} ions. With dimyristoylphosphatidylcholine (DMPC) phospholipid vesicles with 100 μM Ca^{2+} present at 0 °C, significant areas on the i-face of the enzyme showed decreases in the rate of exchange. These areas included regions of residues 3−8, 18−21, and 56−64 which include Tyr-3, Trp-61, Tyr-63, and Phe-64 proposed to penetrate the membrane surface. These regions also contained Phe-5 and Trp-19, proposed to bind the fatty acyl tails of substrate.

The phospholipase A_2 (PLA_2) superfamily consists of 15 different groups and many subgroups that hydrolyze the ester bond of 2-acyl fatty acids from phospholipids (*1, 2*). The products of this reaction, free fatty acids and lysophospholipids, play many different roles as second messengers and precursors for important bioactive molecules (*3*). One of the best-studied PLA_2 enzymes is the cobra (*Naja naja naja*) venom group IA (GIA) PLA_2. This is one of the secreted PLA_2s that are characterized by their low molecular weight, a Ca^{2+} requirement for catalysis, and the presence of seven disulfide bonds. This enzyme is able to hydrolyze monomeric phospholipid substrates, but there is a substantial increase in activity when the enzyme acts on large lipid aggregates (*4*). This enzyme has also been shown to be activated by phospholipids containing phosphatidylcholine headgroups (*5*), and two possible sites for this interaction have been suggested (*6, 7*). Site-directed mutagenesis identified an activator site distinct from the catalytic site (*8*). Extensive kinetic and biophysical studies have been conducted in an effort to understand how soluble enzymes interact with lipid interfaces and to define how the interface affects enzyme kinetics. Many of these studies were carried out on the GI and GII PLA_2s. Thus, the cobra venom GIA PLA_2 has been an important model of not only phospholipid metabolism but also lipid enzymology (*9*).

Biophysical studies on lipid-metabolizing enzymes acting on phospholipids are complicated because this system involves two large macromolecules, the enzyme and the aggregated phospholipid vesicle. The sizes of the lipid aggregates present limitations for many standard biophysical techniques such as solution NMR and X-ray crystallography. For example, many X-ray crystal studies of the secreted PLA_2s have been conducted, including two of the GIA *N. naja naja* enzyme (*6, 10*). These studies were carried out in the presence of metal ions, but not in the presence of large lipid aggregates. Crystallography reports only the state of the enzyme in a crystal, not its state in solution, yet the solution dynamics of the interactions between the PLA_2 and the interface may affect enzyme activity. The *N. naja naja* enzyme has also been studied with NMR in the presence of a monomeric small lipid inhibitor, and a micellar phospholipid analogue (*11, 12*), but no studies have been reported with natural phospholipids. In an attempt to utilize a technique that can yield both structural information in

† This work was supported by NIH Grants GM 20501 (E.A.D.) and CA 099835, CA 118595, and AI 076961 (V.L.W.).

* To whom correspondence should be addressed. E.A.D.: phone, (858) 534-3055; fax, (858) 534-7390; e-mail, edennis@ucsd.edu. V.L.W.: phone, (858) 534-2180; fax, (858) 534-2606; e-mail, vwoods@ucsd.edu.

‡ Department of Chemistry and Biochemistry and Department of Pharmacology.

§ Department of Medicine and Biomedical Science Graduate Program.

10.1021/bi8000962 CCC: $40.75
Published on Web 05/24/2008

solution and information about the dynamics of the enzyme−phospholipid surface interaction, we have employed deuterium exchange mass spectrometry to study PLA_2 lipid−surface interactions and used this technique to add valuable information about these processes.

Peptide amide hydrogen−deuterium exchange analyzed via liquid chromatography−mass spectrometry (DXMS) has been widely used to analyze protein−protein interactions (*13, 14*), protein conformational changes (*15, 16*), protein dynamics (*17*), and protein−lipid interactions (*18*) on proteins lacking disulfide bonds. Tris-carboxyethyl phosphine (TCEP) has regularly been used to reduce proteins containing one or two disulfide bonds, and occasionally more (*19*). However, denaturing and reducing a protein as highly disulfide bonded as the GIA PLA_2 which contains 14 cysteines, all in disulfide bonds, of 119 amino acids are extremely challenging and not previously reported using the DXMS technique. We have now employed DXMS to examine the effects of metal ion binding on solvent accessibility and protein structure. We have probed the structural dynamics of the protein and found large changes in accessibility of the amide hydrogens in heavily disulfide bonded regions of the protein. We have also confirmed the presence of the primary Ca^{2+}-binding site and a secondary Ca^{2+}-binding site. We have also studied the interactions of the soluble GIA PLA_2 with a lipid surface and found a deuterium exchange difference on the interfacial side of the enzyme in the presence of phospholipid vesicles. This has advanced our understanding of the structure and dynamics of the secreted PLA_2s in solution.

MATERIALS AND METHODS

Materials. Cobra venom PLA_2 was purified as described previously (*20*) and stored at −20 °C in 10 mM Tris (pH 7.5). Phospholipids were purchased from Avanti Polar Lipids. All other reagents are analytical reagent grade or better.

On Exchange. D_2O buffer contains 10 mM Tris (pH 7.5) and 50 mM NaCl with or without 1 mM $CaCl_2$ or $BaCl_2$ in 98% D_2O. Hydrogen−deuterium exchange experiments were initiated by mixing 10 μL of 10 mM Tris (pH 7.5) containing 40 μg of GIA PLA_2 with 30 μL of D_2O buffer, producing a final D_2O concentration of 74% at pH 7.5. In the experiments that aimed to examine metal ion binding, the GIA PLA_2 was preincubated with 4 mM $BaCl_2$ or $CaCl_2$ at 22 °C for 5 min. The optimized temperature for separating both fast- and slow-exchanging regions was 22 °C.

The H−D exchange samples were incubated in 22 °C for 15, 60, 600, 3600, and 14400 s at pH 7.5. This gave the greatest distribution of deuterium incorporation over our time course. For the phospholipid experiments, the last time point was dropped. Each time point was repeated three times. The deuterium exchange was quenched via addition of 160 μL of ice-cold quench solution (8 M GdHCl and 1 M TCEP) buffered with formic acid to a pH of 2.5. The samples were placed on ice for 15 min.

Full Exchange. A fully deuterated sample was prepared by adding GIA PLA_2 to a solution of 8 M GdHCl and 1 M TCEP dissolved in 100% D_2O and allowing this to stand at room temperature for 24 h. The GdHCl and TCEP were removed by diluting the solution with 1 volume of 100% D_2O and concentrating the protein with an Amicon Ultra 5000 molecular weight cutoff centrifuge filter (Millipore) at 3000*g* until the volume was half of the original volume. This was repeated 10 times to remove all TCEP and GdHCl. The protein was allowed to sit for 2 h after removal of all denaturants and was then digested under normal conditions.

Off-Line Protein Digestion. To adequately digest the GIA PLA_2, an off-line digestion step had to be added in front of the digestion that occurs during the automated process outlined below. The quenched protein solutions containing 40 μg of protein were added to a 50 μL slurry of ice-cold immobilized pepsin (Pierce Biotechnology) and fungal XIII proteases immobilized on 6% cross-linked agarose beads suspended in 0.8% formic acid and allowed to sit for 15 min. Immobilized fungal XIII protease was prepared as described previously (*16*). This solution was placed in a 5 μm ultrafree-MC centrifugal filter (Millipore) and centrifuged at 700*g* (Eppendorf 5415C centrifuge) to remove the immobilized proteases, and the remaining solution was frozen on dry ice to stop all further amide hydrogen exchange.

Automated Proteolysis−Liquid Chromatography−Mass Spectrometry Analysis of Samples. Samples were then loaded onto the automated DXMS system (*14*) that digested the proteins, separated the peptides, and performed the mass spectrometry analysis. All steps were performed at 0 °C as previously described (*14, 16*). The samples were hand-thawed on melting ice and injected onto a protease column (bed volume of 66 μL) containing porcine pepsin (Sigma; immobilized on Poros 2 AL medium at 30 mg/mL following the manufacturer's instructions, Applied Biosystems), at a flow rate of 100 μL/min with 0.05% (v/v) trifluoroacetic acid (TFA). The eluate from the pepsin column flowed directly onto a C18 column 50 mm in length with an inside diameter of 1.0 mm (Vydac catalog no. 218MS5150). The peptides were eluted with a linear gradient from 0.046% TFA and 6.4% (v/v) acetonitrile to 0.03% TFA and 38.4% acetonitrile at a rate of 50 μL/min. The C18 column eluate flowed directly into a Finnigan LCQ Classic mass spectrometer via its ESI probe operated with a capillary temperature of 200 °C as previously described (*14, 16*).

The presence of large amounts of phospholipid in peptide eluates injected into the mass spectrometer would significantly degrade the peptide analysis. We found that the C18 column employed in the peptide separation bound all of the phospholipids that were carried through the workup in the phospholipid binding experiments. Thus, no extra steps were required to remove it. Up to 10 runs could be completed before the phospholipid bound to the columns began to degrade the peptide separation or yields. After every 10 runs, the HPLC column was flushed with 100% methanol for 30 min to remove the bound phospholipids.

Lipid Preparation and On Exchange. Lipid vesicles were prepared by adding the lipid in chloroform to a small glass tube and evaporating the solvent under argon. The lipid was resuspended in 100 mM KCl at 40 mM and allowed to sit at 50 °C for 30 min. This solution was then bath-sonicated for 10 min. This solution was then size-excluded using 10 passes over a mini extruder (Avanti Polar Lipids) with a 0.03 μm polycarbonate membrane. For lipid binding studies, the enzyme was studied with two different lipid systems, dipalmitoylphosphatidylcholine (DPPC) and dimyristoylphosphatidylcholine (DMPC), and they were used to study lipid binding at 22 and 0 °C, respectively. Experiments were

performed on the gel state of the lipid to prevent excess activity and to prevent the lag phase in activity associated with lipids above the phase transition temperature (*26*). For DPPC experiments, the enzyme was preincubated with 4 mM DPPC SUVs at 22 °C for 5 min with the addition of either 4 mM $BaCl_2$ or 4 mM EDTA. This gave total concentrations after addition of deuterium of 1 mM DPPC and 1 mM $BaCl_2$ or EDTA.

For DMPC experiments, the enzyme was preincubated with 4 mM DMPC SUVs at 0 °C in the presence of 100 μM Ca^{2+} to minimally activate the enzyme. A modified version of the Dole assay (*8*) using the exact same conditions that were used for deuterium exchange experiments was used to assay enzyme activity. Deuterium exchange results were obtained for only time points with <10% hydrolysis of lipid vesicles to prevent acidification of exchange buffer and effects of non-phospholipid−lipid aggregates. The enzyme was preincubated with 4 mM DMPC lipid vesicles with 400 μM Ca^{2+} for 30 s at 0 °C. This gave a total concentration after dilution by the addition of deuterated buffer of 1 mM DMPC and 100 μM Ca^{2+}. The K_d of the enzyme for lipid vesicles at 40 °C is 4.4 mM, but lipid concentrations of >1 mM were limited by the amount of protein required for mass spectrometry analysis. The mole ratio of lipid molecules to protein molecules in the samples was ~16:1.

Data Processing. SEQUEST (Thermo Finnigan Inc.) was used to assign peptide sequences to the ion peaks eluting from the C18 column from their MS/MS spectra. Peaks that SEQUEST identified were then analyzed with DXMS Explorer (Sierra Analytica Inc., Modesto, CA) as previously described (*14, 16*). All peptides selected for analysis had to first pass the quality-control thresholds setup in the DXMS software and then were manually checked. If the same peptide was found with different charges (1, 2, or 3), the one with the best signal-to-noise ratio was selected for analysis. The mass of the peptide was determined by measuring the centroid of the isotopic envelope of the peptide. The level of deuterium on a given peptide is expressed as the incorporated deuteron number (Inc#). The incorporated deuteron number is the difference between the centroids of a given peptide in nondeuterated and deuterated samples. The extent of back-exchange was ~35−50% due to the long digestion time but was corrected using the fully deuterated control experiments. The deuteration level (D) is the ratio of the Inc# of the sample to the Inc# of a fully deuterated sample given by the following equation (*21*).

$$D = \frac{m_s - m_{0\%}}{m_{100\%} - m_{0\%}} N$$

where m_i is the centroid of the peptide exposed to sample conditions (s), on exchange quench control (0%), and fully deuterated (100%) and N is the deuterium level measured before correction.

Deuterium that has been incorporated into the amides of an intact protein is rapidly lost from the very rapidly exchanging amino-terminal proton and most N-terminal amide protons of peptides created under exchange quench conditions. Thus, in our experiments, no hydrogen exchange information is available for the first two amino acids of a probe peptide. We use the term region to represent all amides where we can track deuterium incorporation. In some cases, we specifically state the peptide identity as shown by mass spectrometry and label those as peptides (*14, 16*). Regions of exchange were calculated by subtracting overlapping peptide fragments as described in previous work (*22*). Reported percent changes are calculated as the difference in exchange between conditions over the total number of deuterons in a region.

RESULTS

Protein Digestion of GIA PLA_2. GIA PLA_2 is a very rigid protein due to its small size (13500 Da) and the presence of seven disulfide bonds. Because of this, finding conditions for digesting the protein was a major hurdle to obtaining a good peptide map. TCEP has been employed to reduce disulfide bonds under the low-pH conditions needed for deuterium exchange quenching (*19*). In our initial experiments, we added TCEP under a variety of conditions to the chromatographic solvents employed with the pepsin column in the automated DXMS system. This met with no success. We found that significant digestion could be achieved only by predigesting the enzyme with pepsin and fungal XIII protease prior to loading the samples onto the automated DXMS system described in Materials and Methods. The predigestion was achieved by quenching protein samples in a solution containing 1 M TCEP and 8 M GdHCl for 15 min followed by dilution into a solution containing immobilized pepsin and fungal XIII proteases for 15 min. This solution was then loaded onto the automated DXMS system and run through another immobilized pepsin column before being loaded onto the C18 column. Back-exchange levels of ~50% were found with this technique, but by using fully deuterated controls, the amount of back-exchange could be measured and used to determine corrected deuterium levels.

Using these conditions, 55 good-quality peptides were identified. If peptides occurred in more than one charge state, we show only the one with the best signal-to-noise ratio. This reduced the number of useful ions with no redundant data to 45, which are shown in Figure 1. This map covers 96% of the protein and has a high degree of overlap, allowing for the determination of deuterium levels for regions of the protein smaller than the corresponding peptide. The difference in deuterium levels of the two overlapping peptides is the number of deuterons associated with the unmatched amino acids. This allows us to determine the deuteration levels of regions of the protein smaller than either peptide.

This map was generated in the presence of both metal ions and lipid without any changes in the number and intensity of peptide fragments. The number of deuterons incorporated was measured for all 55 peptides, including peptides with multiple charge states, but to simplify the graphics, only 23 of the peptides, those shown with thick lines in Figure 1, were chosen to generate the deuterium exchange data for all of the other figures. However, all 55 peptides were analyzed in each experiment to make sure that the exchange data agreed with those of the 21 selected peptides.

Deuterium Exchange of GIA PLA_2. On exchange experiments were carried out on the native GIA PLA_2 employing the DXMS methods outlined above. Figure 2 shows deuterium exchange percentages for these experiments. Figure 2 is divided into 17 different regions. The deuterium levels of each region were generated by analyzing several overlapping

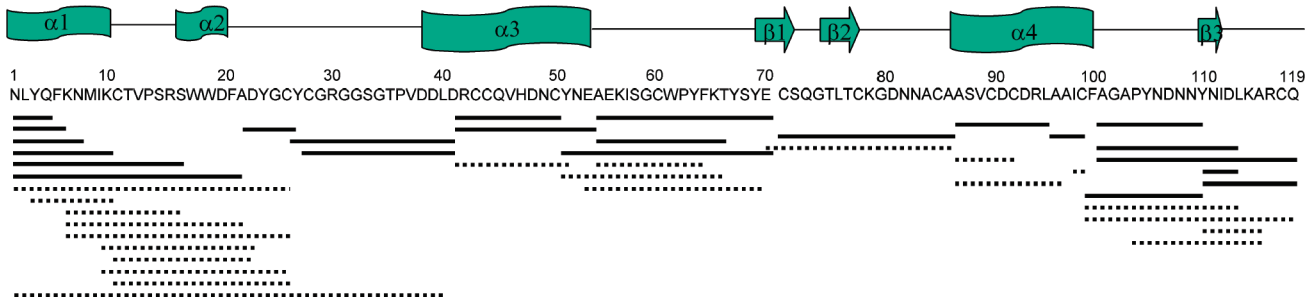

FIGURE 1: Pepsin-digested peptide coverage map of the GIA PLA_2 sequence with α-helical (α) and *β*-sheet (*β*) regions indicated. Black lines represent peptides chosen for this study. Dotted lines represent peptides that were identified and analyzed but were used only as a comparison for the peptides denoted with solid line. There are 45 distinct peptides which were studied with only one selected for peptides that have multiple charge states.

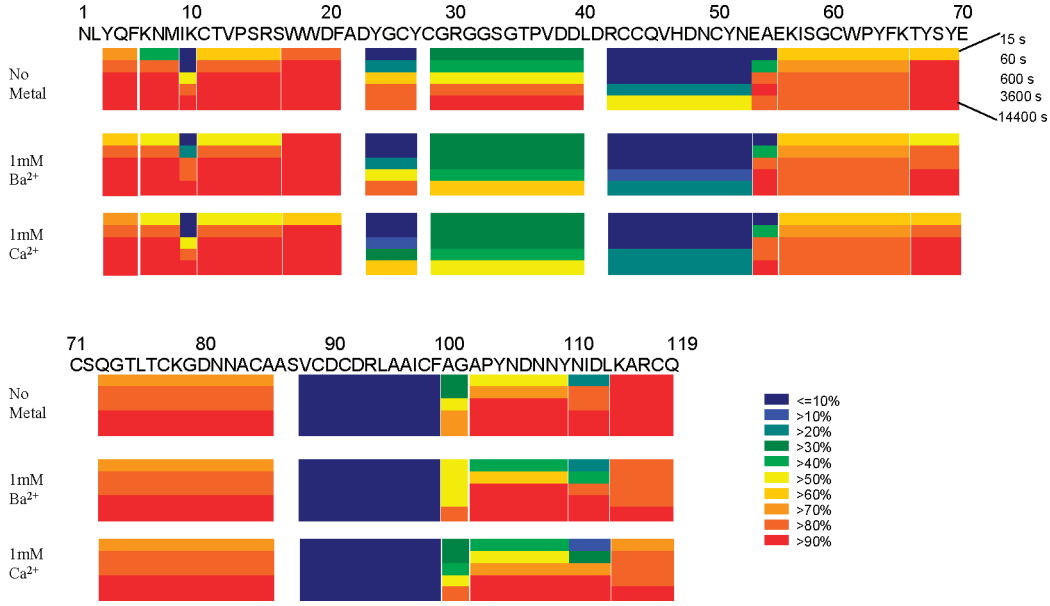

FIGURE 2: Amide hydrogen−deuterium exchange analysis of the effect of calcium and barium on GIA PLA_2. The deuterium exchange map with and without Ba^{2+} and Ca^{2+} is shown with the amino acid sequence of the GIA PLA_2. Each condition is divided into rows corresponding to each time point, from 15 s to 240 min from top to bottom. Colors indicate the amounts of H−D exchange in a given time period.

peptides that allowed us to measure the deuteration level of the smallest protein regions possible.

The data show that both the N- and C-terminal regions (residues 1−23 and 102−119, respectively) of the protein exchange very rapidly (Figure 2). The first 23 amino acids encompass the first α-helix and exhibit more than 80% deuteration within the first minute of on exchange with the exception of amino acids 9 and 10. The region of residues 9 and 10 exchanges much slower and does not reach 80% deuteration until 60 min. This region encompasses the last two residues of the first α-helix and is next to the disulfide bond bridging residues 11 and 71 as shown in Figure 3. This may explain the decreased rate of exchange. The C-terminal area stretching from amino acid 102 to 119 also exhibits more than 80% deuteration within the first minute of on exchange.

The region encompassing amino acids 56−86, which contains the two antiparallel *β*-sheets, also exhibits very rapid exchange with deuteration rates comparable to those seen in both the N- and C-termini. The region from residue 24 to 40 is less flexible than the N- and C-termini and takes 60 min to fully exchange. In contrast, the rates of exchange on α-helices of residues 39−55 and 84−101 are very slow. The region from residue 89 to 101 exchanges less than 10% even after 24 h of on exchange. The region from amino acid 43 to 53 does exchange, but at a level of only 50% after 4 h.

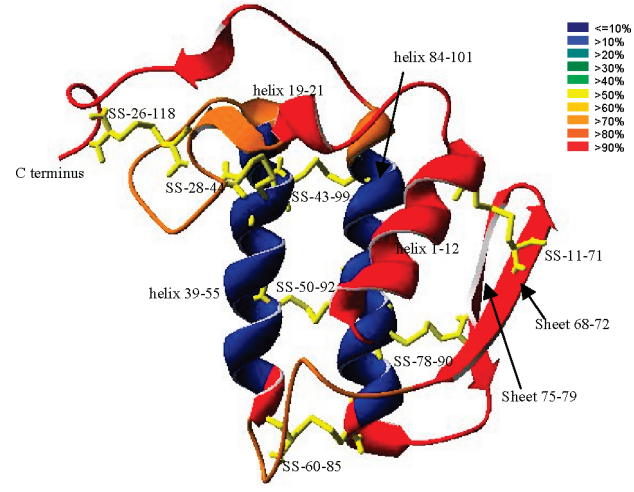

FIGURE 3: Deuteration level of GIVA PLA_2 visualized on the crystallographic model of the *N. naja naja* enzyme (PDB entry 1PSH). The deuterium exchange map of GIVA PLA_2 after 3000 s of on exchange is shown with the colors indicating the exchange rates detected by DXMS. Disulfide bonds are colored yellow.

Changes in Deuterium Exchange of GIA PLA_2 When Ba^{2+} or Ca^{2+} Is Bound. The GIA PLA_2 requires Ca^{2+} for activity

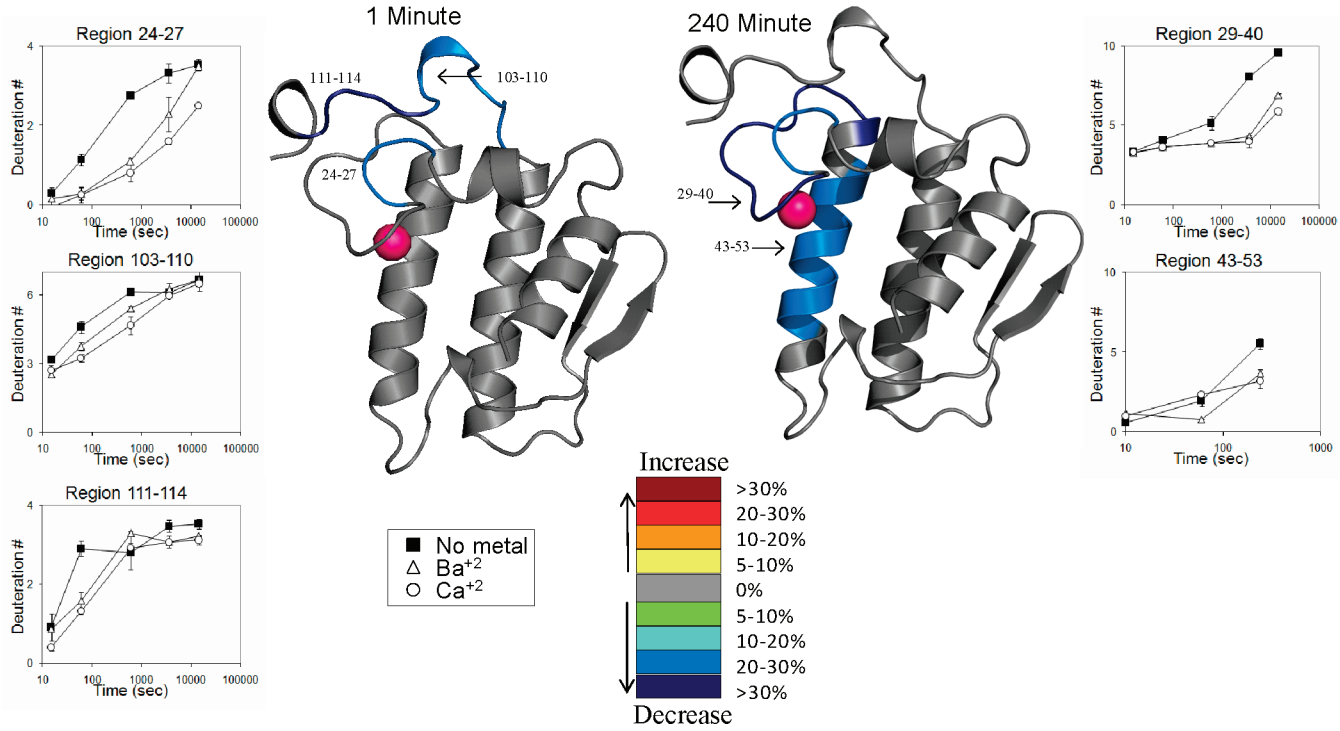

FIGURE 4: Deuterium exchange of the GIA PLA_2 upon metal binding. The numbers of incorporated deuterons at five time points are plotted for regions that show changes upon either calcium or barium (or both) binding. The changes in deuterium exchange are shown at two different time points mapped on the *N. naja naja* GIA PLA_2 crystal structure (PDB entry 1PSH) with the calcium ion colored pink. Colors denote the changes in the deuterium level.

with one molecule binding in the catalytic site. A second Ca^{2+} may also bind to the enzyme, but its role in activity has not been defined. Ba^{2+} also binds to the primary Ca^{2+} binding site in the catalytic site, but it inhibits activity, although it does produce similar structural changes in the enzyme as detected by UV−vis spectroscopy (*23*). Thus, we measured deuterium on exchange of the GIA PLA_2 from 15 s to 4 h in the presence of 1 mM $BaCl_2$ or $CaCl_2$ to ascertain if these metals produce different exchange patterns. Several areas in GIA PLA_2 show changes in deuterium exchange in the presence of Ca^{2+}. Three of these, residues 24−27, 29−40, and 43−53 (Figure 4), are part of the primary Ca^{2+}-binding site of the GIA PLA_2 which consists of the backbone oxygens of Y27, G29, and G31 and the aspartic acid oxygens of D48 (*10*). Thus, Ca^{2+} binding appears to decrease the level of deuterium exchange seen in regions of residues 24−27, 29−40, and 43−53. Interestingly, the decrease in the level of deuterium exchange in regions of residues 29−40 and 43−50 appears to mainly affect slow-exchanging amide hydrogens. This is shown by the greatest difference in deuterium exchange being seen from 3000 to 10000 s (Figure 4).

One other region consists of residues 103−114, where the changes affect only fast-exchanging amide hydrogens with no difference seen after 60 min of on exchange. Since these residues are not part of the primary Ca^{2+}-binding site, these results would be consistent with a second Ca^{2+}-binding site. The crystal structures of the structurally related *Naja naja atra* GIA PLA_2 have shown such a secondary Ca^{2+}-binding site with contacts between Asn-112 and Asp-23 and a secondary Ca^{2+} ion (*24*). Via comparison of the structures of these two enzymes, which are superimposable in this region, and when the exchange data are overlaid, it is clear

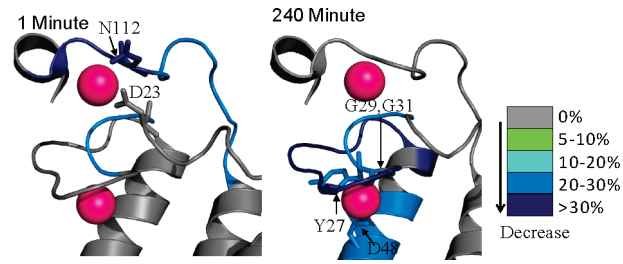

FIGURE 5: Crystal structure of the *N. naja atra* GIA PLA_2 with a secondary calcium site present and the calcium ions colored pink. The deuterium exchange data from *N. naja naja* PLA_2 were overlaid onto the *N. naja atra* structure (PDB entry 1POA) for two time points. Amino acids involved in binding the calcium ions are labeled. Color denote the changes in the deuterium level.

that a Ca^{2+} binding to this second site in the *N. naja naja* PLA_2 would account for the exchange data (Figure 5).

The rates of exchange with Ba^{2+} are essentially the same for residues 29−40, 111−114, and 43−53. Ba^{2+} also causes changes in residues 103−110 and 24−27, although the magnitude of these changes is not as great as with Ca^{2+}.

These changes in exchange obviously have important structural implications because Ba^{2+} seems to bind the same sites, but in such a way that it inactivates the enzyme. These results are consistent with a picture in which Ba^{2+} binds competitively for the Ca^{2+}-binding site. The affinities of Ba^{2+} and Ca^{2+} are different with K_d values of 0.15 and 0.4 mM, respectively (*23*), and these differences in affinity may explain the difference in exchange seen at the Ca^{2+}-binding sites.

Deuterium Exchange of GIA PLA_2 in the Presence of Lipid. One of the main goals of this research was to determine if deuterium exchange could yield information about how the soluble GIA PLA_2 interacts with large substrate aggregates.

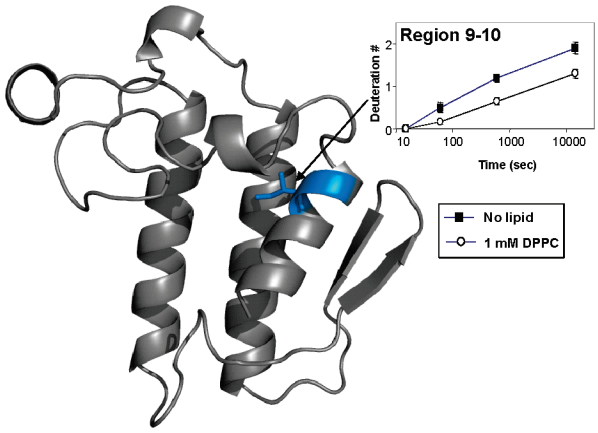

FIGURE 6: Deuterium exchange of the GIA PLA_2 with areas of decreased exchange upon phospholipid binding in the presence of 1 mM EDTA. The number of incorporated deuterons at four time points is plotted for residues 9 and 10. Changes were mapped onto the *N. naja naja* GIA PLA_2 crystal structure (PDB entry 1A3D).

To that end, deuterium exchange of GIA PLA_2 at time points varying from 15 s to 1 h was analyzed in the presence of 1 mM small unilamellar vesicles (SUVs) of DPPC. These experiments were carried out in the absence of Ca^{2+} to prevent hydrolysis of the phospholipid vesicles. EDTA was included to ensure that no free Ca^{2+} was present. Previous work in our laboratory has shown very low levels of enzyme binding to phospholipid without metal present but that either Ca^{2+} or Ba^{2+} increased this level of phospholipid binding (*25*). For this reason, experiments were also carried out using Ba^{2+} (data not shown) as a replacement for Ca^{2+}, which achieved the exact same exchange patterns that were seen with lipid in the absence of metal ions. Studies were conducted at 22 °C because it has been shown that the GIA PLA_2 has a significant lag phase with lipid above the phase transition temperature (*26*), so we desired our lipid surface to be only in the gel state. Most regions of the GIA PLA_2 show no change in deuterium exchange in the presence of DPPC lipid vesicles, except for one small region of the protein. This area consists of amino acids Ile-9 and Lys-10 (Figure 6). The deuteration level of residues 9 and 10 was calculated by subtracting the deuterium levels of peptide 1−8 from that of peptide 1−10; the same decrease in the level of exchange with lipid is seen in five other peptides (1−17, 1−21, 1−27, 5−21, and 5−27) that include residues 9 and 10. This effect is not seen in peptides 9−21, 9−17, 11−21, and 9−27 which do not include residues 9 and 10 (noting that the first two amino acids fully exchange with the technique and are not included in the analysis). This shows that the effect is strictly limited to the region of amino acids 9 and 10. There is a 20−30% change between the lipid-free and DPPC-containing protein samples.

Further experiments were conducted using 100 μM Ca^{2+} with phospholipid vesicles to minimally activate the enzyme. Original experiments using DPPC vesicles with 100 μM Ca^{2+} at 22 °C caused high levels of phospholipid hydrolysis. Further experiments were conducted at 0 °C to further slow hydrolysis, so the total level of phospholipid hydrolysis stayed below 10% over the deuterium on exchange time course. Due to the change in temperature, the lipid used was shifted from DPPC to DMPC. The phase transition temperatures of DPPC and DMPC are 41 and 23 °C, respectively, so we used DMPC at 0 °C to view a similar physical state of the lipid that was seen in DPPC studies at 22 °C. Activity assays performed showed that at 300 s the enzyme had not hydrolyzed more then 10% of the lipid surface. Four regions of the protein, namely, residues 3−5, 6−8, 18−21, and 56−64, had significant decreases in their levels of exchange upon exposure to lipid in the presence of calcium (Figure 7). Deuterium content for residues 6−8 was calculated via subtraction of the value of peptide 1−5 from that of peptide 1−8, and the deuterium content of residues 18−21 was calculated via subtraction of the value of peptide 1−17 from that of peptide 1−21.

Regions of residues 3−5 and 6−8 are part of the first α-helix located on the i-face of the enzyme. Due to multiple overlapping peptides in this region, we were able to localize changes in this helix. The largest change was seen for residues 3−5 containing Tyr-3 and Phe-5 and had a 20−30% decrease in the level of exchange over all time points. Interestingly, from using peptide overlap data from peptides 1−4 and 1−5, it seems that both amino acids 3 and 4 and amino acid 5 have independent decreases in the level of exchange. Residues 3 and 4 had a smaller decrease in exchange at 100 and 300 s, with residue 5 having a constant deuterium decrease. Residues 6−8 also had a 10−20% decrease in the level of exchange. Residues 18−21 had a 5−10% decrease in the level of exchange, and this region includes Trp-18 and Trp-19. Residues 56−64 had a 10−20% decrease in the level of exchange until 100 s, with less than 10% at 300 s. Residues 9 and 10 which had a decrease in the level of exchange with lipid and no Ca^{2+} present at 22 °C (Figure 6) had zero on exchange at 0 °C up to 300 s, so no change could be detected with lipid in the presence of Ca^{2+} at these lower temperatures. Importantly, this experiment shows interaction of the phospholipid with the i-face of the protein and demonstrates the potential of deuterium exchange mass spectrometry in studying proteins that catalyze reactions at the lipid surface.

DISCUSSION

There are many crystal structures of GIA PLA_2, but these structures show only a static picture of the enzyme under crystallization conditions. Using deuterium exchange mass spectrometry, we are able to study the protein in solution under varying conditions. This represents the first use of deuterium exchange mass spectrometry to probe the structure of a PLA_2 and its interaction with a lipid surface. In this study, we show a region of the protein that is solvent accessible blocked from exchange by extensive disulfide bonds, the presence of a secondary Ca^{2+}-binding site in the *N. naja naja* GIA PLA_2, and the ability to probe lipid−lipase interactions with deuterium exchange mass spectrometry.

The on exchange experiments with the native GIA PLA_2 showed that the three α-helices exhibited dramatically different exchange rates. The N-terminal helix exchanges vary rapidly, while the two core helices exhibit almost no exchange even though they are on the surface of the protein and at least some of the amide protons should be accessible to water. The difference is that helices of residues 39−55 and 84−101 are involved in four disulfide bonds with other parts of the protein while the N-terminus is not. Other regions that are not involved in extensive disulfide bonding also show very fast deuterium exchange rates which would be expected

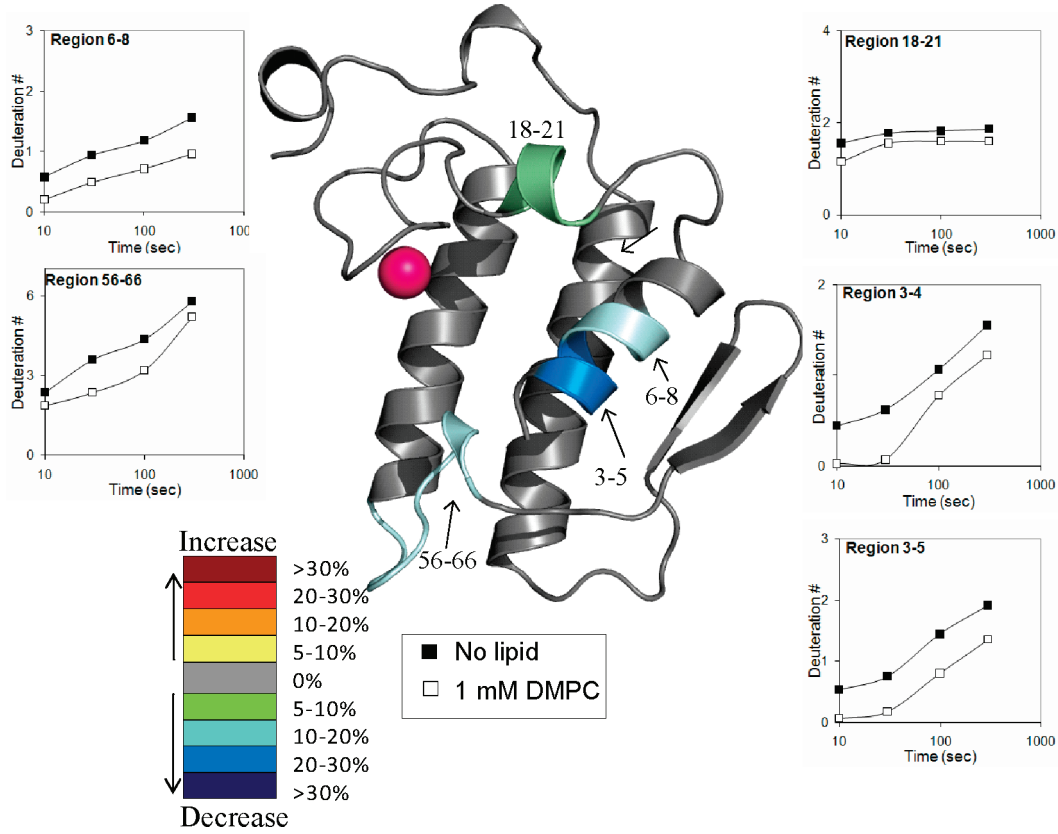

FIGURE 7: Deuterium exchange of the GIA PLA_2 upon DMPC vesicle binding at 0 °C in the presence of 100 μM Ca^{2+}. The numbers of incorporated deuterons at four time points are plotted for regions that show changes upon DMPC binding. The changes in deuterium exchange are shown mapped on the *N. naja naja* GIA PLA_2 crystal structure (PDB entry 1PSH) with the calcium ion colored pink. Colors denote the changes in the deuterium level.

for such a small solvent-exposed protein. Studies performed on a recombinant macrophage colony stimulating factor-β with nine disulfide bonds (six intramolecular and three intermolecular) did not reveal this same lack of deuterium exchange in surface-exposed disulfide bonding areas (*19*). That study concluded that exchange rates were mainly due to solvent accessibility. The exchange rates of α-helices in this protein were correlated with the depth from solvent rather then conformational constraints from disulfide bonds. This protein is a dimer of two 221-amino acid subunits that is quite large and contains nine disulfide bonds. The difference in the exchange rates between this protein and GIA PLA_2 exists because of the higher percentage of disulfide bonds in this protein and the localization of these bonds intertwined with the two α-helices. The amino acids participating in disulfide bonds are shown in Figure 3 with six of the cysteine residues located on the two helices. This is a novel finding as it has not previously been demonstrated that extensively disulfide bonded areas of proteins are held extremely rigidly by those bonds and that exchange with the solvent is restricted.

Because of this tight disulfide bond structure, the protein is very resistant to both digestion and denaturation and needed extreme conditions to fragment the protein. This extremely tight disulfide-bonded network is a possible evolutionary adjustment in toxin-containing PLA_2s to protect against protease digestion in the venom or in their prey. Our use of a predigestion with TCEP was necessary to achieve these results and provides a procedure for investigating other highly disulfide bonded proteins.

Two crystal structures of the *N. naja naja* GIA PLA_2 have been previously determined by our laboratory (*6, 10*). In both of these crystals, the enzyme was present as trimers. The *N. naja atra* GIA PLA_2 structure was determined as a dimer and contained two Ca^{2+}-binding sites per enzyme molecule (*24*). The structure of *N. naja naja* of Fremont et al. (*10*) contained Ca^{2+} in the primary binding site but did not show this secondary Ca^{2+}. However, the trimer structure is held together by an intermolecular salt bridge between Arg-30 on one monomer and Asp-23 on a second monomer. Asp-23 is one of the essential residues in binding the secondary Ca^{2+} as shown in the *N. naja atra* crystal. This trimer interaction occurs at high enzyme concentrations and may block the incorporation of the secondary Ca^{2+} ion. We could not isolate Asp-23 in the DXMS analysis because of the lack of overlap of peptides in this region.

The C-terminal region from residue 103 to 114 also forms part of the secondary site. This region does show a decrease in the level of exchange that would suggest the presence of Ca^{2+} in this site. This indicates that when the enzyme is in solution, Ca^{2+} is bound to the second site and that the lack of the second Ca^{2+} in the original crystal structure was due to the trimer contacts with Asp-23. If a model is generated with the *N. naja naja* crystal structure containing a Ca^{2+} ion in the secondary Ca^{2+}-binding site shown in the *N. naja atra* structure, the amino acids are in the correct position for Ca^{2+} binding.

Ba^{2+} showed decreases in the level of deuterium exchange as did Ca^{2+}, but the magnitude of the change was smaller. Decreases in the level of deuterium exchange at the Ca^{2+}-

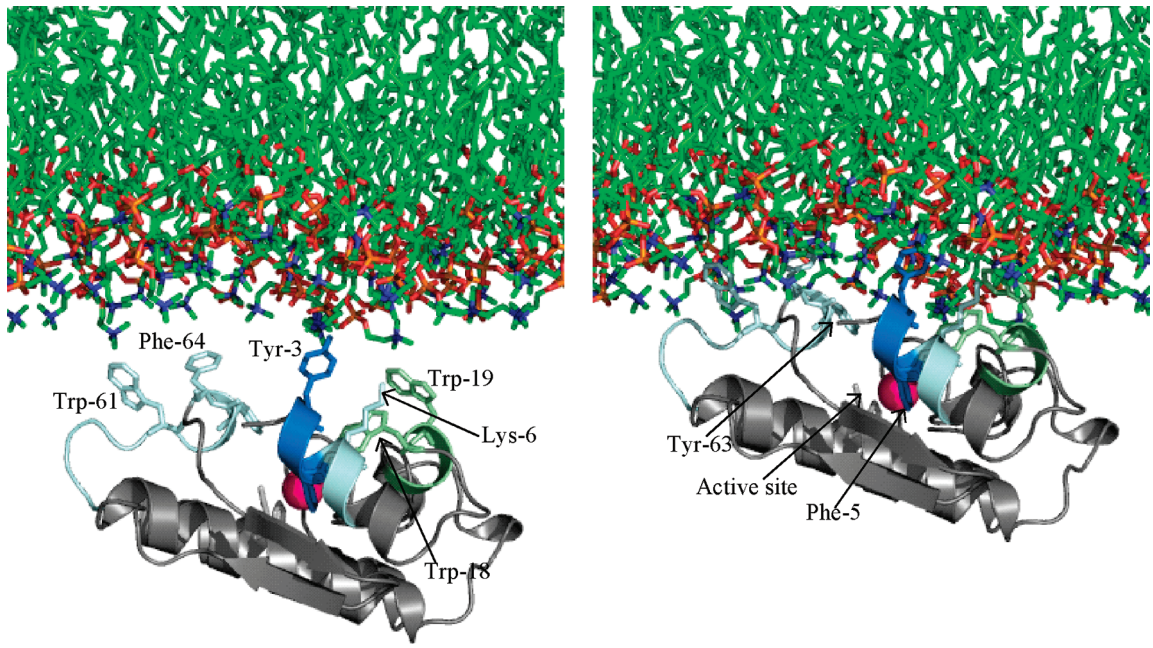

FIGURE 8: Hypothetical model of GIA PLA_2 binding to a DMPC membrane surface (left) before associating with the membrane and (right) after association with the membrane. Areas with decreases in the level of exchange have been colored, and amino acid residues Tyr-3, Phe-5, Lys-6, Trp-18, Trp-19, His-47, Trp-61, Tyr-63, Phe-64, and Asp-93 have been drawn in stick form. This figure was created with PyMol.

binding sites were smaller in the presence of Ba^{2+} than at the same levels of Ca^{2+}. This is most likely due to the different affinities of these ions for the enzyme of 0.15 mM for Ca^{2+} and 0.4 mM for Ba^{2+} (*23*). These results suggest that Ba^{2+} binds in exactly the same place as the Ca^{2+} ion, but there are differences in the affinity at the site of binding.

The interfacial activation of PLA_2 has been an area of interest for many years. The use of DPPC vesicles without Ca^{2+} present to probe lipid binding did not show changes in deuterium exchange in large areas of the protein. However, there was a distinct effect at residues 9 and 10. This region contains isoleucine 9, which has been postulated to be one of the residues in the hydrophobic core in the active site of the protein based on the crystal structure (*24, 27*). This change in deuterium exchange may well be the interaction of the sn-2 fatty acid from the phospholipid with the hydrophobic residue.

Experiments caried out in the presence of low levels of Ca^{2+} with DMPC SUVs showed significant decreases in the level of exchange in large areas of the enzyme proposed to bind the membrane interface. A hypothetical scheme of membrane binding of the *N. naja naja* GIA PLA_2 is shown in Figure 8.

Our experiments showed decreases in the level of exchange at regions containing Tyr-3, Trp-61, Tyr-63. and Phe-64. We propose that the aromatic residues here are inserting into the membrane bilayer. Mutations of the aromatic amino acids have been tested in the structurally similar *N. naja atra* GIA PLA_2 enzyme and found to significantly diminish interfacial activation (*28*). Similar experiments in the *N. naja naja* GIA enzyme showed mutations at Trp-61, Tyr-63, and Phe-64 also significantly reduced the extent of interfacial inactivation (*8*). Our experiments also show a decrease in residues 6−8 containing Lys-6, which is in the correct orientation to interact with phosphate headgroups of the membrane surface. Experiments using the GIA PLA_2 inhibitor manoalide showed that reaction of manoalide with Lys-6 caused a large decrease in activity, maybe inducing an incorrect protein orientation at the surface (*29*). The deuterium exchange data suggest that the majority of the interactions between the enzyme and the interface are mediated by residues 3−8 and 56−64. The area of residues 18−21 has a very small change in exchange compared to changes seen for residues 3−8 and 56−64. We propose that binding to a lipid surface is mediated by the aromatic and charged residues in these areas and blocks them from solvent exposure. Our experiments confirm that these areas of the enzyme are interacting with the membrane surface, but only upon exposure to Ca^{2+}.

Our experiments also demonstrate a decrease for regions containing Phe-5, Ile-9, and Trp-19. We propose these amino acids are mediating binding of the fatty acyl tails of the phospholipid substrate. Previous NMR studies carried out by our laboratory using an amide substrate analogue dispersed in micelles showed differences in Leu-2, Phe-5, Trp-19, Ala-22, and Phe-100 with GIA PLA_2 (*12*). A crystal structure of the *N. naja atra* enzyme with an inhibitor bound showing hydrophobic interactions among Leu-2, Phe-5, Ile-9, Trp-19, and Tyr-69 also exists (*27*). Our deuterium exchange results very closely match the results seen in both inhibitor-bound GIA PLA_2s. In our studies, we were not able to isolate Leu-2, Ala-22, or Phe-100 due to very slow exchange in these regions, or a lack of resolution. The changes seen at Ile-9 and Phe-5 have a constant decrease in the level of exchange at all time points, where regions proposed to penetrate the membrane surface have smaller decreases in the level of exchange at later time points. This suggests that substrate binds very tightly and blocks this area from on exchange at all time points, while the enzyme may hop on and off substrate, allowing surface-penetrating residues to exchange at later time points.

CONCLUSION

This study shows rigidification of the two extensively disulfide bonded helices, and the presence of a secondary Ca^{2+}-binding site present in the *N. naja naja* group IA PLA_2. Also, we have shown that both of these sites show changes upon Ba^{2+} binding, but not at the same levels of exchange. This study also shows an interaction between the soluble enzyme and the lipid surface at both surface and substrate binding regions of the protein. This study marks a novel use of deuterium exchange mass spectrometry in the study of lipid−lipase interactions as well as the use of novel digestion and denaturation methods to work with very highly disulfide bonded proteins.

ACKNOWLEDGMENT

We are extremely grateful to Dr. (Howard) Yuan-Hao Hsu for critical discussions about this work.

REFERENCES

1. Six, D. A., and Dennis, E. A. (2000) The Expanding Superfamily of Phospholipase A_2 Enzymes: Classification and Characterization. *Biochim. Biophys. Acta 1488*, 1–19.
2. Schaloske, R. H., and Dennis, E. A. (2006) The Phospholipase A_2 Superfamily And Its Group Numbering System. *Biochim. Biophys. Acta 1761*, 1246–1259.
3. Balsinde, J., Balboa, M. A., Insel, P. A., and Dennis, E. A. (1999) Regulation and Inhibition of Phospholipase A_2. *Annu. Rev. Pharmacol. Toxicol. 39*, 175–189.
4. Plückthun, A., Rohlfs, R., Davidson, F. F., and Dennis, E. A. (1985) Short-Chain Phosphatidylethanolamines: Physical Properties and Susceptibility of the Monomers to Phospholipase A_2 Action. *Biochemistry 24*, 4201–4208.
5. Adamich, M., Roberts, M. F., and Dennis, E. A. (1979) Phospholipid Activation of Cobra Venom Phospholipase A_2. II. Characterization of the Phospholipid-Enzyme Interaction. *Biochemistry 18*, 3308–3313.
6. Segelke, B. W., Nguyen, D., Chee, R., Xuong, N. H., and Dennis, E. A. (1998) Structures of Two Novel Crystal Forms of *Naja naja naja* Phospholipase A_2 Lacking Ca^{2+} Reveal Trimeric Packing. *J. Mol. Biol. 279*, 223–232.
7. Ortiz, A. R., Pisabarro, M. T., Gallego, J., and Gago, F. (1992) Implications of a consensus recognition site for phosphatidylcholine separate from the active site in cobra venom phospholipases A_2. *Biochemistry 31*, 2887–2896.
8. Lefkowitz, L. J., Deems, R. A., and Dennis, E. A. (1999) Expression of Group IA Phospholipase A_2 in *Pichia pastoris*: Identification of a Phosphatidylcholine Activator Site Using Site-Directed Mutagenesis. *Biochemistry 38* (43), 14174–14184.
9. Deems, R. A., Eaton, B. R., and Dennis, E. A. (1975) Kinetic Analysis of Phospholipase A_2 Activity Toward Mixed Micelles and Its Implications for the Study of Lipolytic Enzymes. *J. Biol. Chem. 250*, 9013–9020.
10. Fremont, D. H., Anderson, D., Wilson, I. A., Dennis, E. A., and Xuong, N.-H. (1993) The Crystal Structure of Phospholipase A_2 from Indian Cobra Reveals a Novel Trimeric Association. *Proc. Natl. Acad. Sci. U.S.A. 90*, 342–346.
11. Plesniak, L. A., Boegeman, S. C., Segelke, B. W., and Dennis, E. A. (1993) Interaction of Phospholipase A_2 with Thioether Amide Containing Phospholipid Analogues. *Biochemistry 32*, 5009–5016.
12. Plesniak, L., Yu, L., and Dennis, E. A. (1995) Conformation of Micellar Phospholipid Bound to the Active Site of Phospholipase A_2. *Biochemistry 34*, 4943–4951.
13. Mandell, J. G., Falick, A. M., and Komives, E. A. (1998) Identification of protein-protein interfaces by decreased amide proton solvent accessibility. *Proc. Natl. Acad. Sci. U.S.A. 95*, 14705–14710.
14. Hamuro, Y., Anand, G. S., Kim, J. S., Juliano, C., Stranz, D. D., Taylor, S. S., and Woods, V. L., Jr. (2004) Mapping intersubunit interactions of the regulatory subunit (RIα) in the type I holoenzyme of protein kinase A by amide hydrogen/deuterium exchange mass spectrometry (DXMS). *J. Mol. Biol. 340*, 1185–1196.
15. Hoofnagle, A. N., Resing, K. A., Goldsmith, E. J., and Ahn, N. G. (2001) Changes in protein conformational mobility upon activation of extracellular regulated protein kinase-2 as detected by hydrogen exchange. *Proc. Natl. Acad. Sci. U.S.A. 98*, 956–961.
16. Brudler, R., Gessner, C. R., Li, S., Tyndall, S., Getzoff, E. D., and Woods, V. L., Jr. (2006) PAS domain allostery and light-induced conformational changes in photoactive yellow protein upon I2 intermediate formation, probed with enhanced hydrogen/deuterium exchange mass spectrometry. *J. Mol. Biol. 363*, 148–160.
17. Wales, T. E., and Engen, J. R. (2006) Hydrogen exchange mass spectrometry for the analysis of protein dynamics. *Mass Spectrom. Rev. 25*, 158–170.
18. Man, P., Montagner, C., Vernier, G., Dublet, B., Chenal, A., Forest, E., and Forge, V. (2007) Defining the interacting regions between apomyoglobin and lipid membrane by hydrogen/deuterium exchange coupled to mass spectrometry. *J. Mol. Biol. 368*, 464–472.
19. Yan, X., Zhang, H., Watson, J., Schimerlik, M. I., and Deinzer, M. L. (2002) Hydrogen/deuterium exchange and mass spectrometric analysis of a protein containing multiple disulfide bonds: Solution structure of recombinant macrophage colony stimulating factor-β (rhM-CSFβ). *Protein Sci. 11*, 2113–2124.
20. Hazlett, T. L., and Dennis, E. A. (1985) Affinity Chromatography of Phospholipase A_2 from *N. naja naja* (Indian Cobra) Venom. *Toxicon 23*, 457–466.
21. Zhang, Z., and Smith, D. L. (1993) Determination of amide hydrogen exchange by mass spectrometry: A new tool for protein structure elucidation. *Protein Sci. 2*, 522–531.
22. Del Mar, C., Greenbaum, E. A., Mayne, L., Englander, S. W., and Woods, V. L., Jr. (2005) Structure and properties of α-synuclein and other amyloids determined at the amino acid level. *Proc. Natl. Acad. Sci. U.S.A. 102*, 15477–15482.
23. Roberts, M. F., Deems, R. A., and Dennis, E. A. (1977) Spectral Perturbations of the Histidine and Tryptophan in Cobra Venom Phospholipase A_2 Upon Metal Ion and Mixed Micelle Binding. *J. Biol. Chem. 252*, 6011–6017.
24. Scott, D. L., White, S. P., Otwinowski, Z., Yuan, W., Gelb, M. H., and Sigler, P. B. (1990) Interfacial catalysis: The mechanism of phospholipase A2. *Science 250*, 1541–1546.
25. Roberts, M. F., Deems, R. A., and Dennis, E. A. (1977) Dual Role of Interfacial Phospholipid in Phospholipase A_2 Catalysis. *Proc. Natl. Acad. Sci. U.S.A. 74*, 1950–1954.
26. Kensil, C. R., and Dennis, E. A. (1979) Action of Cobra Venom Phospholipase A_2 on the Gel and Liquid Crystalline States of Dimyristoyl and Dipalmitoyl Phosphatidylcholine Vesicles. *J. Biol. Chem. 254*, 5843–5848.
27. White, S. P., Scott, D. L., Otwinowski, Z., Gelb, M. H., and Sigler, P. B. (1990) Crystal structure of cobra-venom phospholipase A2 in a complex with a transition-state analogue. *Science 250*, 1560–1563.
28. Stahelin, R. V., and Cho, W. (2001) Differential roles of ionic, aliphatic, and aromatic residues in membrane-protein interactions: A surface plasmon resonance study on phospholipases A2. *Biochemistry 40*, 4672–4678.
29. Ghomashchi, F., Yu, B. Z., Mihelich, E. D., Jain, M. K., and Gelb, M. H. (1991) Kinetic characterization of phospholipase A2 modified by manoalogue. *Biochemistry 30*, 9559–9569.

BI8000962